

REDUCED ORDER AEROELASTIC MODEL FOR RAPID DYNAMIC LOADS ANALYSIS

B. A. Winther* and M. L. Baker†

The Boeing Company, Long Beach, California 90807

A rapid dynamic loads analysis capability is an essential tool for the design of load alleviation systems. We present a unique technique based on a state variable formulation that eliminates the need for auxiliary states, i.e., lag terms, to represent the oscillatory aerodynamic forces. The analysis technique was developed in Ref. 1 and is used here to derive the output equations for structural loads caused by atmospheric turbulence and/or control surface inputs. Results generated by application of these loads equations are evaluated through comparison with MSC/Nastran solutions in the frequency domain. In addition to the design of load alleviation systems, the present rapid analysis technique may be used for identification of critical load conditions and for synthesis of flight control laws in general.

Nomenclature

$A' A'' B$	= matrices in state equations of motion
$C' C'' D$	= matrices in loads output equation
F	= aerodynamic force vector
M	= mass matrix in MFP axes system
P	= total dynamic load matrix
P'	= load matrix due to elastic response
P''	= load matrix due to system input
U	= mean airflow velocity
X, Y, Z	= aircraft body axes coordinates
a'	= in-phase aero matrix in MFP system
a''	= out-of-phase aero matrix in MFP system
d	= modal displacement vector
e	= state variable vector in MFP axes system
f, g, h	= aircraft displacements in MFP system
p, q, r	= aircraft angular rates about body axes
q_d	= dynamic pressure
u, v, w	= aircraft linear rates along body axes
α'	= in-phase aero matrix along body axes
α''	= out-of-phase aero matrix along body axes
β	= matrix of input forces
δ_c	= control surface rotational displacement

ε	= state variable vector in body axes system
γ	= structural damping matrix
η	= vector of inputs
κ	= structural stiffness matrix
μ	= mass matrix in body axes system
ω	= circular frequency

Subscripts

m, n	= modal indices
g	= gust component
i	= input component index
j	= load component index

Superscripts

(\cdot)	= $d(\cdot)/dt$
T	= transposed vector

Introduction

Some transport aircraft concepts currently being studied are extremely lightweight and flexible compared to traditional designs. The feasibility of the new concepts may depend on flight control systems to alleviate the structural loads. Development of this type of advanced system requires an analysis technique that is efficient enough to enable rapid batch simulation without sacrificing the accuracy necessary for control law design.

Ref. 1 describes a state space formulation that eliminates the need for lag terms to represent the unsteady aerodynamics. Comparisons with more elaborate solution techniques have shown excellent correlation for structural response data such as accelerations, rates and

* Senior Principal Engineer, A&T Loads and Dynamics. Associate Fellow AIAA.

† Senior Engineer, A&T Loads and Dynamics. Member AIAA.

displacements due to control surface excitation. We will further develop this analysis technique by deriving output equations for the structural loads due to various inputs. The following section provides a brief summary of the basic state space formulation.

Equations of Motion

It is customary in stability and control applications to describe the equations of motion in a body axes system that is fixed relative to the aircraft center of gravity and with the X-axis oriented along the initial wind axis (also named stability axis). In the disciplines of dynamic loads and flutter, however, the convention is to use a mean flight path (MFP) axes system that is aligned with the initial (unperturbed) flight path of the aircraft and moving with its average velocity relative to an earth-fixed system. Practically all analyses of structural dynamics consider only level flight, i.e., the gravity force is assumed balanced by the unperturbed lift of the aircraft. Ref. 6 (pp. 863-864) contains a detailed discussion of transformations between these two and other common coordinate systems. In the present paper we will apply the body axes system with X positive forward and Z positive down. It should be noted that the orientation of our body axes system is the conventional one², but that it differs from the one used in Ref. 6.

The aircraft equations of motion as derived in Ref. 1 may be written in the following form:

$$\dot{\boldsymbol{\varepsilon}} = \mathbf{A}'\dot{\boldsymbol{\varepsilon}} + \mathbf{A}''\boldsymbol{\varepsilon} + \mathbf{B}\boldsymbol{\eta} \quad (1.1)$$

where $\boldsymbol{\eta}$ is a vector of inputs and $\boldsymbol{\varepsilon}$ denotes the displacement component of the state variable vector. For longitudinal (symmetric) motion the input vector $\boldsymbol{\eta}$ and the rate component of $\boldsymbol{\varepsilon}$ are defined by:

$$\begin{aligned} \dot{\boldsymbol{\varepsilon}} &= (u, w, q, \dot{\delta}_c, \ddot{\delta}_c, \ddot{\delta}_c, \dot{w}_g, \ddot{w}_g)^T \\ \boldsymbol{\eta} &= (\delta_c, \dot{\delta}_c, \ddot{\delta}_c, w_g, \ddot{w}_g)^T \end{aligned} \quad (1.2)$$

The p-transform technique^{1,3} requires the "global" \mathbf{A}' , \mathbf{A}'' and \mathbf{B} matrices to be assembled in an iterative manner based on linear approximations of the unsteady aerodynamic forces:

$$\mathbf{F}(\omega) \approx \mathbf{a}'\mathbf{e} + \mathbf{a}''\dot{\boldsymbol{\varepsilon}} \quad (1.3)$$

where \mathbf{e} denotes the displacement component of the state variable vector in the MFP axes system. The piecewise linear approximations in the frequency domain are applied in narrow intervals that correspond to eigen-

values of the combined \mathbf{A}' and \mathbf{A}'' matrices. Results of this approximation are at least as accurate as those obtained with higher order representations covering a wide frequency band. The salient feature, of course, is that this accuracy is gained without increasing the number of equations to be solved.

Transformation to Body Axes

Routines for computation of unsteady aerodynamic forces, e.g., the doublet-lattice method⁵, generally require the motion of the aircraft to be described in the MFP axes system. For the case of longitudinal motion, the mean axes (rigid body) degrees of freedom are defined by:

$$\mathbf{e}_n = (f, h, \theta)^T \quad n = 1, 2, 3 \quad (2.1)$$

where f denotes fore-aft motion, h represents plunge motion and θ symbolizes pitch about a reference axis located near the center of gravity. The f and θ degrees of freedom are the same whether measured in the MFP axes system or in the body axes system. The transformation between the two systems is ruled by the equations:

$$\begin{aligned} u &= \dot{f} \\ w &= \dot{h} + U\theta \\ q &= \dot{\theta} \end{aligned} \quad (2.2)$$

As a result of the transformation, the first three columns ($n=1, 2, 3$ for all values of m) of the mass matrix \mathbf{M} and the aerodynamic matrices \mathbf{a}' and \mathbf{a}'' in the MFP axes system are replaced by:

$$\mu_{m,n} = \mathbf{M}_{m,n} + q_d \omega^{-2} \mathbf{a}'_{m,n} \quad \text{for } n = 1, 2 \quad (2.3)$$

$$\mu_{m,3} = \mathbf{M}_{m,3} + q_d \omega^{-2} (\mathbf{a}'_{m,3} - U \mathbf{a}''_{m,2}) \quad (2.4)$$

$$\mathbf{a}'_{m,n} = 0 \quad \text{for } n = 1, 2, 3 \quad (2.5)$$

$$\mathbf{a}''_{m,n} = \mathbf{a}''_{m,n} \quad \text{for } n = 1, 2 \quad (2.6)$$

$$\alpha''_{m,3} = \mathbf{a}''_{m,3} + U(\omega^{-2} \mathbf{a}'_{m,2} + \mathbf{M}_{m,2} / q_d) \quad (2.7)$$

The remaining parts of the mass and aerodynamic matrices are identical in the two axes systems and so are the stiffness and structural damping matrices.

In each of the frequency intervals where the approximation of Eq. (1.3) is applied, the "local" A' , A'' and B matrices are computed from:

$$\begin{aligned} A' &= \mu^{-1}(\alpha'' - \gamma) \\ A'' &= \mu^{-1}(\alpha' - \kappa) \\ B &= \mu^{-1}\beta \end{aligned} \quad (2.8)$$

Global A' , A'' , and B matrices are then assembled in the iterative manner that was alluded to above and that is described in Ref. 1. The elements of the β -matrix in eq. (2.8) are defined by:

$$\beta_{m,i} = (\alpha'_{m,i}, \alpha''_{m,i}, -\mu_{m,i}) \quad (2.9)$$

where the subscripts correspond to state variable "m" and input component "i". The part of β corresponding to gust inputs has only two columns since the mass contribution is zero.

Calculation of Dynamic Loads

Aerodynamic loads on an aircraft component may be calculated by selecting appropriate auxiliary displacement functions, d_m , that serve as weighting factors for the pressure distribution, Δp_n , in the generalized force integral. The in-phase portion, for instance, is defined by:

$$a'_{m,n} = \frac{2}{\rho U^2} \int d_m \operatorname{Re}(\Delta p_n) dS \quad (3.1)$$

Thus, hinge moments are obtained by selecting auxiliary rotation modes of one radian for the control surfaces. Similarly, the aerodynamic contribution to the wing bending moment is calculated by considering a roll displacement about the wing root chord.

The total structural load component, P_j , derived from the auxiliary mode "j", consists of two parts:

$$P_j = P'_j + P''_j \quad (3.2)$$

In eq. (3.2) the first term represents dynamic loads caused by the elastic response of the airframe and the second term denotes loads generated directly by the atmospheric turbulence and/or control surface inputs. After applying the transformation to body axes as prescribed by Eq. (2.2) we obtain:

$$\begin{aligned} P'_j &= \alpha'_j \varepsilon + \alpha''_j \eta - \mu_j \beta \\ P''_j &= \beta_j \eta \end{aligned} \quad (3.3)$$

Combination of Eqs. (3.3) and (1.1) yields the following canonical form of the loads output equation:

$$P = C' \varepsilon + C'' \eta + D \eta \quad (3.4)$$

where the matrices C' , C'' and D are composed of the following row components:

$$\begin{aligned} C'_j &= \alpha''_j - \mu_j A' \\ C''_j &= \alpha'_j - \mu_j A'' \\ D_j &= \beta_j - \mu_j B \end{aligned} \quad (3.5)$$

In the following section these equations are applied to a sample problem and evaluated by correlation with data derived from MSC/Nastran⁷.

Evaluation of Method

The present reduced-order modeling technique, also referred to as the p-transform, was evaluated through comparison with MSC/Nastran frequency domain solutions. Figs. 1-2 show corresponding acceleration responses for an advanced transport aircraft flying at sea level and at a Mach number of 0.4. We observe that the two solution techniques yield practically identical magnitude results up to a frequency of 7.0 Hz. Discrepancies above that frequency are explained by differences in the modeling of the elevator surface. A rigid control surface mode is used to generate the p-transform input whereas a more realistic, flexible elevator model provides the excitation force in the MSC/Nastran analysis. We note that the first torsion mode of the elevator produces a sharp peak in the acceleration response slightly below 10.0 Hz. The phase response error evident in the frequency band 4-6 Hz (fig. 2), confirms the observation made in Ref. 1 that the p-transform phase data are less accurate in those parts of the spectrum where the magnitude is small.

The predicted loads due to control surface motion show equally good agreement between the two methods. Figs. 3-4 are representative of the magnitude and phase comparisons obtained for elevator inputs. These results are generated at the same fuel, payload and flight conditions used in the sample problem discussed above. Again, minor discrepancies that are observed at higher frequencies are attributed to differences in the structural modeling of the control surface.

The analyses presented above validate the p-transform technique for the dynamics due to aircraft motion-induced forces. A general time domain method, however, also requires the response due to atmospheric turbulence to be predicted in an accurate manner. We applied gust excitation forces to the same model used for the elevator inputs and, as before, we compared results generated by the p-transform technique with data from the MSC/Nastran program. Fig. 5 shows the real part of a frequency response due to random turbulence with the amplitude one ft/sec. We note that the accuracy of the p-transform deteriorates above a frequency of two Hz. This discrepancy is caused by rapid variation of the gust excitation forces over the frequency band.

To achieve improved accuracy in the turbulence response it may be necessary to apply a Rational Function Approximation technique^{8,9,10} for the gust input terms. In many cases, however, the accuracy demonstrated here may be sufficient, especially for preliminary design purposes. This argument is supported by the observation that the power of atmospheric turbulence is attenuated rapidly with frequency. Fig. 6 presents a Power Spectral Density (PSD) comparison of vertical acceleration at the pilot station due to a gust input of one ft/sec. The gust power distribution is modeled by the Dryden spectrum in both analyses. We note that the p-transform prediction for the acceleration PSD is reasonably accurate. The corresponding loads are not as accurate, however, as exemplified by Fig. 7 showing a comparison of two computed PSDs for the aft fuselage bending moment.

Concluding Remarks

A rapid dynamic loads analysis capability based on the p-transform technique was developed and evaluated through comparisons with MSC/Nastran solutions in the frequency domain. Our analyses demonstrated that the elastic responses as well as the structural loads caused by control surface motion were predicted accurately. The same level of accuracy, however, was not obtained for responses and loads due to atmospheric turbulence. Even though the p-transform accuracy for the gust loads may be sufficient for preliminary design applications, we recommended a modification to the approximation for the gust excitation forces. There are several options for improving the approximation. One method developed by other investigators is the Rational Function

Approximation that introduces lag terms to describe the input forces due to turbulence. We plan to further investigate this approach in the near future.

References

- ¹ Winther, B. A., Goggin, P. J. and Dykman, J. R., "Reduced Order Dynamic Aeroelastic Model Development and Integration with Nonlinear Simulation", AIAA/ASME/ASCE/AHS/ASC 39th Conference on Structures, Structural Dynamics and Materials, Paper AIAA-98-1897, Long Beach, California, April 1998.
- ² Etkin, B., *Dynamics of Flight*, Wiley, New York, 1959.
- ³ Heimbaugh, R. M., "Flight Controls Structural Dynamics IRAD", McDonnell Douglas Report MDC-J2303, March 1983.
- ⁴ Albano, E. and Rodden, W. P., "A Doublet-Lattice Method for Calculating Lift Distributions on Oscillating Surfaces in Subsonic Flow", *AIAA Journal*, Vol. 7, pp. 279-285, Feb 1969.
- ⁵ Giesing, J. P., Kalman, T. P. and Rodden, W. P., "Subsonic Unsteady Aerodynamics for General Configurations", Air Force Flight Dynamics Laboratory Report AFFDL-TR-71-5, Nov 1971..
- ⁶ Winther, B. A., Hagemeyer, D. A., Britt, R. T., and Rodden, W. P., "Aeroelastic Effects on the B-2 Maneuver Response", *Journal of Aircraft*, Vol. 32, No. 4, 1995, pp. 862-867.
- ⁷ Rodden, W. P. (ed.), "MSC/NASTRAN Handbook for Aeroelastic Analysis", MacNeal-Schwendler Corp., MSR-57, Los Angeles, CA, Nov 1987.
- ⁸ Dykman, J., "An Approximate Transient Gust Force Derived from Phase Shifted Rational Function Approximations to the Doublet-Lattice Harmonic Gust Coefficients", McDonnell Douglas Report MDC-92-K0283, Feb 1992.
- ⁹ Goggin, P. J., "A General Gust and Maneuver Load Analysis Method to Account for the Effects of Active Control Saturation and Nonlinear Aerodynamics", AIAA Dynamics Specialist Conference Paper No. 92-2126, Dallas, Texas, April 1992.
- ¹⁰ Tiffany, S. H. and Adams, W. H., "Nonlinear Programming Extensions to Rational Function Approximation Methods for Unsteady Aerodynamic Forces", NASA Technical Paper 2776, July 1988.

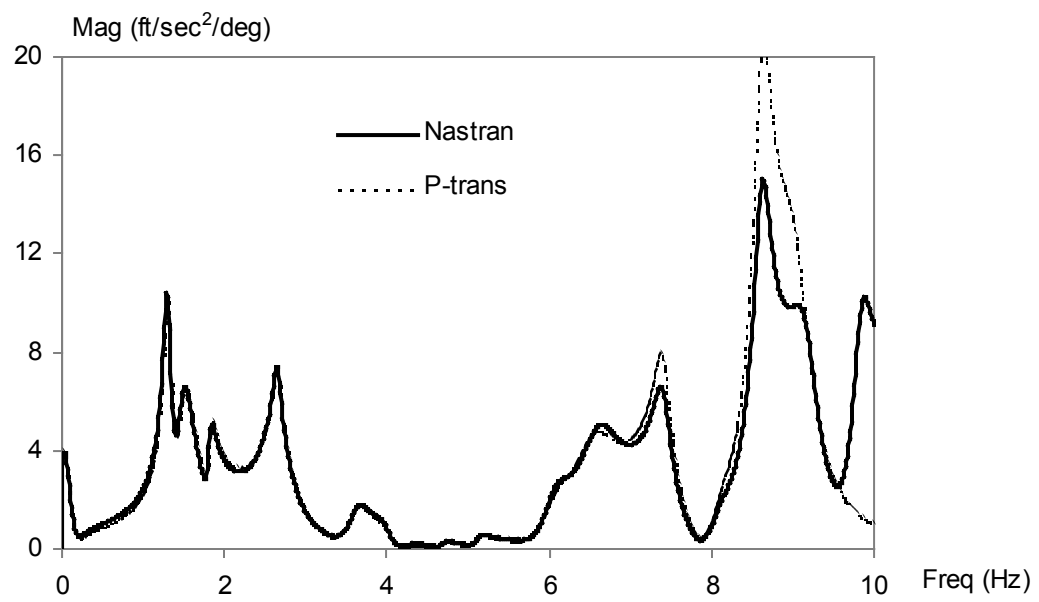


Fig 1. Magnitude of Vertical Acceleration at Pilot Station due to Elevator Excitation.

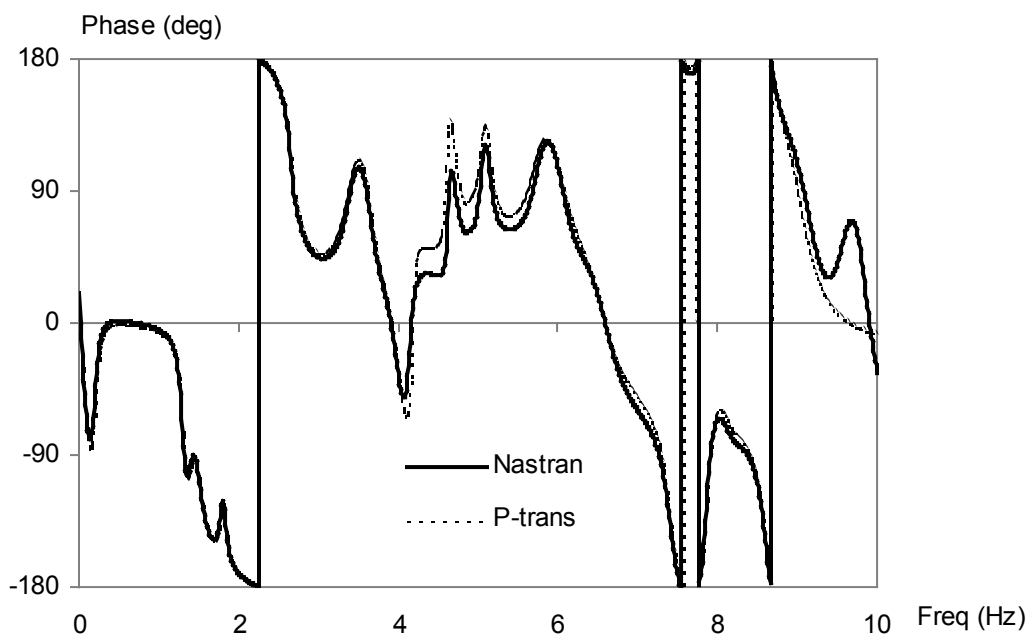


Fig 2. Phase of Vertical Acceleration at Pilot Station due to Elevator Excitation.

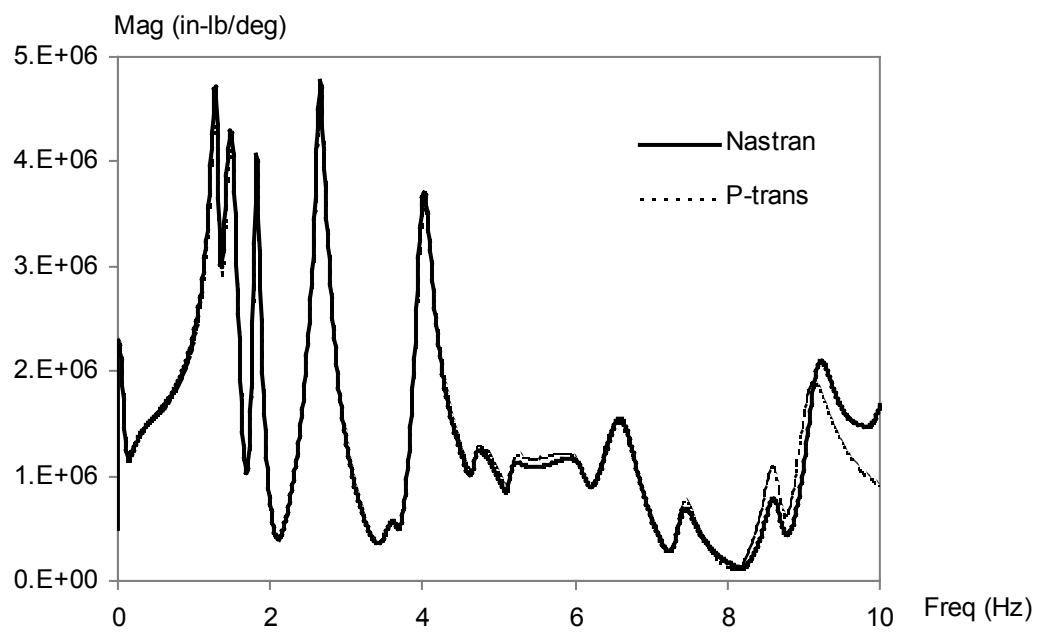


Fig 3. Magnitude of Aft Fuselage Bending Moment due to Elevator Excitation.

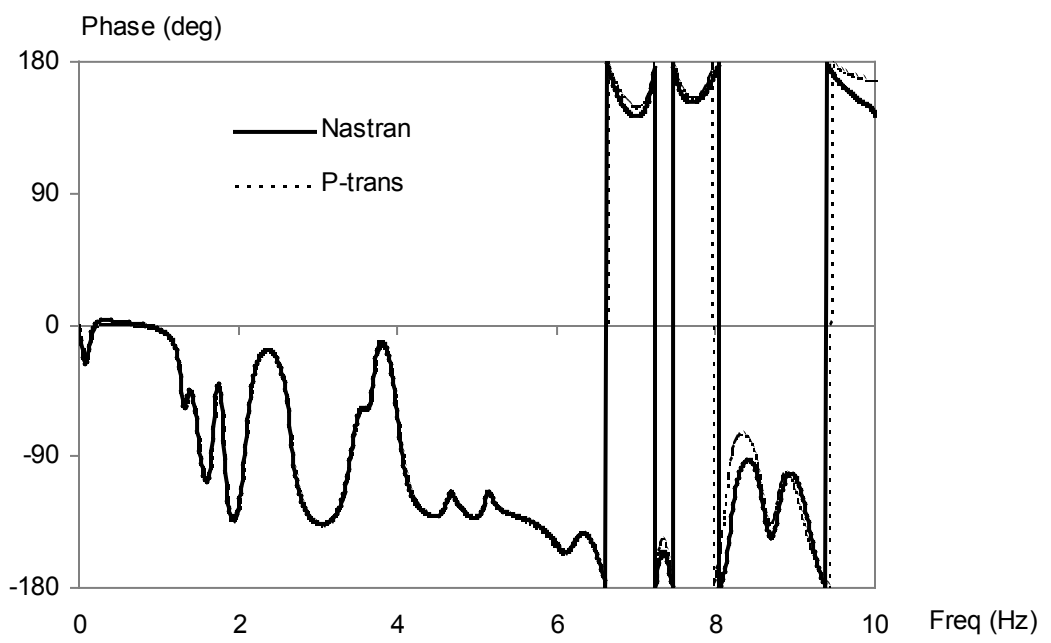


Fig 4. Phase of Aft Fuselage Bending Moment due to Elevator Excitation.

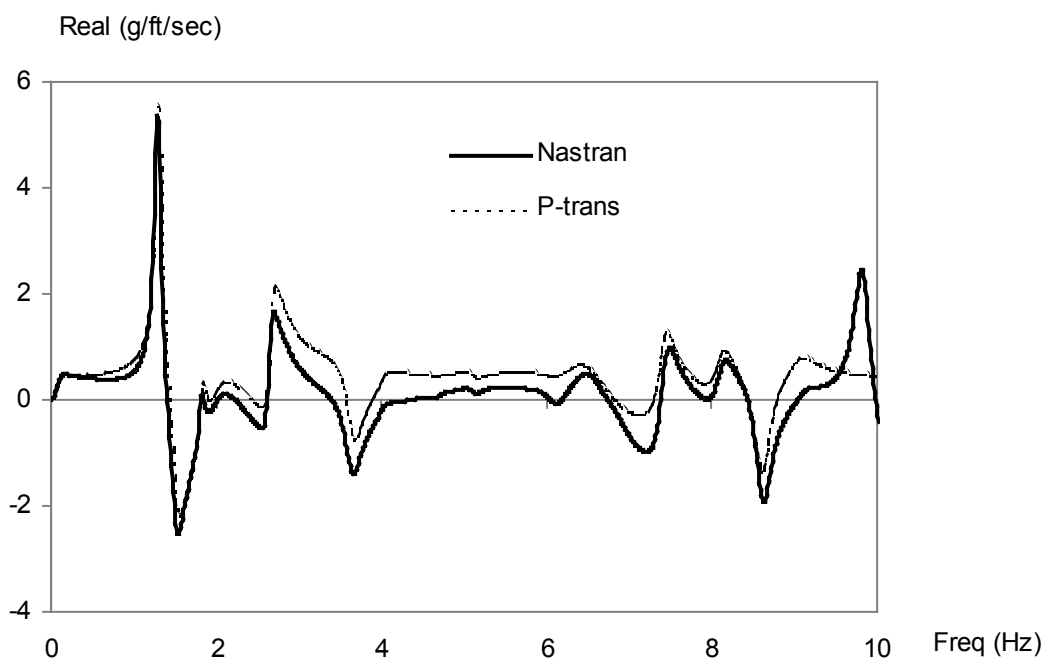


Fig 5. In-phase Part of Vertical Acceleration at Pilot Station due to Gust

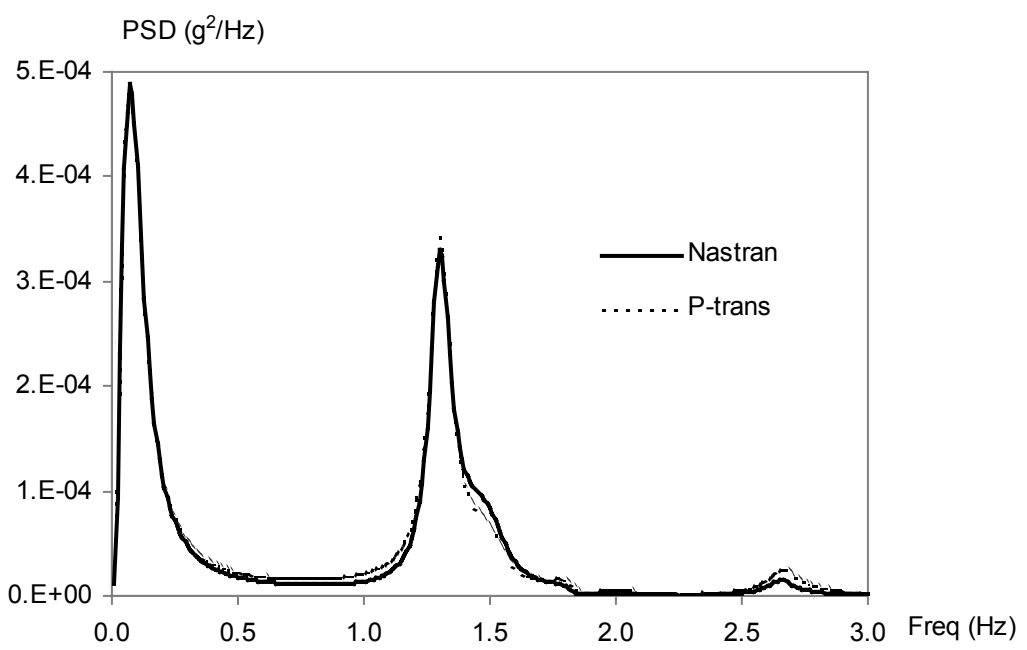


Fig 6. PSD of Vertical Acceleration at Pilot Station due to Gust

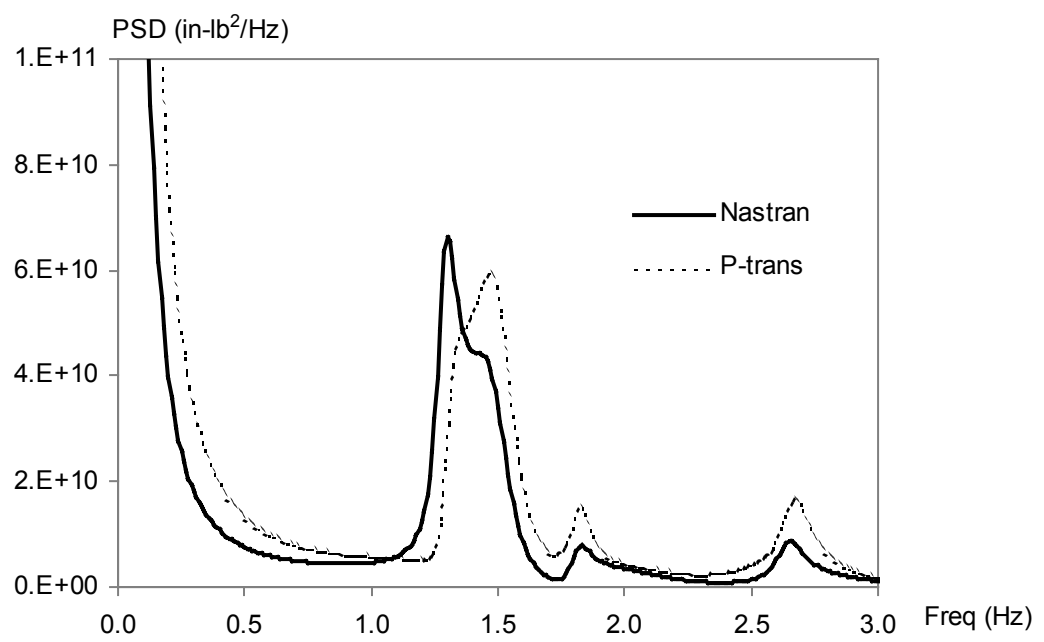


Fig 7. PSD of Aft Fuselage Bending Moment due to Gust.

